1   **Title:** Intergenerational transmission of the patterns of functional and structural brain

2   networks

3

4   **Authors and addresses:**

5   Yu Takagi[1,2*], Naohiro Okada[1,3], Shuntaro Ando[1,4], Noriaki Yahata[1,5,6], Kentaro Morita[1,7],

6   Daisuke Koshiyama[1], Shintaro Kawakami[1], Kingo Sawada[8], Shinsuke Koike[1,9], Kaori Endo[10],

7   Syudo Yamasaki[4], Atsushi Nishida[4], Kiyoto Kasai[1,3], Saori C Tanaka[2]

8

9   [1] Department of Neuropsychiatry, Graduate School of Medicine, University of Tokyo, Tokyo,

10   Japan

11   [2] ATR Brain Information Communication Research Laboratory Group, Kyoto, Japan

12   [3] International Research Center for Neurointelligence (WPI-IRCN), University of Tokyo

13   Institutes for Advanced Study (UTIAS), University of Tokyo, Tokyo, Japan

14   [4] Department of Psychiatry and Behavioral Science, Tokyo Metropolitan Institute of Medical

15   Science, Tokyo, Japan

16   [5] Institute for Quantum Life Science, National Institutes for Quantum and Radiological Science

17   and Technology, Chiba, Japan

18   [6] Department of Molecular Imaging and Theranostics, National Institute of Radiological

19   Sciences, National Institutes for Quantum and Radiological Science and Technology, Chiba,

20   Japan

21   [7] Department of Rehabilitation, University of Tokyo Hospital, Tokyo, Japan

22   [8] Office for Mental Health Support, Mental Health Unit, Division for Practice Research, Center

23   for Research on Counseling and Support Services, University of Tokyo, Tokyo, Japan

24   [9] University of Tokyo Institute for Diversity and Adaptation of Human Mind (UTIDAHM),

25   University of Tokyo, Tokyo, Japan

26   [10] Unit for Mental Health Promotion, Research Center for Social Science & Medicine, Tokyo

27   Metropolitan Institute of Medical Science, Tokyo, Japan

28

29   *****Corresponding author**: yutakagi322@gmail.com (Yu Takagi, Ph.D.)

30   **Competing Interests**: The authors declare no competing interests.

31

## Abstract

There is clear evidence of intergenerational transmission of life values, cognitive traits, psychiatric disorders, and even aspects of daily decision making. To investigate biological substrates of this phenomenon, brain has received increasing attention as a measurable biomarker and potential target for intervention. However, no previous study has quantitatively and comprehensively investigated the effects of intergenerational transmission on functional and structural brain networks from parents to their children. Here, by employing an unusually large cohort dataset, we show that patterns of functional and structural brain networks are preserved over a generation. We also demonstrate that several demographic and behavioural phenotypes have effects on brain similarity. Collectively, our results provide a comprehensive picture of neurobiological substrates of parent-child similarity, and demonstrate the usability of our dataset for investigating the neurobiological substrates of intergenerational transmission.

46

## Introduction

There is clear evidence of intergenerational transmission of socio-economic status[1], intelligence[2], personality[3], parenting style[4], job-selection[5], and psychiatric disorders[6]. This correspondence between parents and their children is not confined to the period in which children are young and live with their parents, but is found over the course of their lives[7]. Although genetic and non-genetic environmental effects are clearly transferred to children from their parents, the mechanisms of parent-child similarity are poorly understood[8].

In recent years, brain has received increasing attention as a target for monitoring and intervention because genetic and epigenetic effects occur at the molecular level and are distal from complex behaviour[9]. Several previous studies have shown that functional connectivity (FC or edge) during wakeful rest obtained by functional magnetic resonance imaging (fMRI) is associated with individual differences in diverse cognitive traits[10–19]. In parallel to functional brain information, individual differences in brain structure have also been characterised and related to diverse cognitive traits[20]. Importantly, previous studies have reported that grey matter volume (GMV) at specific locations in the brain is associated with individual differences in cognitive traits[20–24].

In addition to individual differences in cognitive traits, previous studies also showed that FC[25–43] and GMV[25,44–57] are heritable. These studies have typically used genome wide association study (GWAS) or family/twin study. Most studies have assessed the genetic effects on each edge- or region-level, i.e. univariate analysis, and typically considered demographic or behavioural information as covariates. Importantly, previous studies have not directly focused on the effects of intergenerational transmission from parents to their children.

More recent studies have started to directly examine the effects of intergenerational transmission on the brain using datasets of parent-child dyads[8,59–62]. For example, Lee et al. and Yamagata et al. investigated the similarity of parent-child dyads in FC and GMV, respectively[59,62]. However, these studies involved several limitations. First, no study has quantitatively compared the similarity of different brain networks in detail. Second, because none of these studies examined both functional and structural data together, it remains unclear how functional and structural information are interrelated. Third, no study has comprehensively investigated the effects of demographic and behavioural effects on

77    similarity. Overall, it is currently unclear whether, to what extent, and how the brains of
78    parent-child dyads are similar. This situation has arisen, in part, because investigating the
79    above questions requires a large number of parent-child dyads to provide neuroimaging
80    datasets with rich behavioural phenotypes. Furthermore, such an approach requires a formal
81    analytical framework with rigorous statistical analyses and rich computational resources.

82          In the current study, we sought to understand the neurobiological substrates of
83    parent-child similarity by combining a statistical framework that allowed us to investigate
84    network-level similarities and a rich dataset from a subsample of a large population-based
85    longitudinal cohort (N = 84 parent-child dyads) consisting of resting-state fMRI, structural MRI,
86    and behavioural phenotypes of parents and their children[63,64]. We sought to answer several
87    questions: Can a parent-child dyad be identified based on their brains? If so, which brain
88    networks are more similar compared with other networks? Is the similarity solely driven by
89    functional or structural information? How do demographic and behavioural factors affect
90    brain similarity?

91          Using a dataset consisting of parents and their children, we quantitatively
92    investigated the brain similarity of parent-child dyads in detail. The present findings
93    demonstrated that it is possible to reliably identify a parent-child dyad based on the similarity
94    of their brains. This effect was not solely driven by either functional or structural brain
95    similarity alone: although functional and structural information had comparable accuracy,
96    they exhibited important differences, and played complementary roles. Children's basic
97    demographic factors, including age and sex, testosterone level, and questionnaire-based
98    developmental scores affected parent-child brain similarity. Collectively, our results provide a
99    detailed picture of how the brains of children and their parents are similar, and demonstrate
100    the usability of our unique cohort dataset for investigating the neurobiological substrates of
101    intergenerational transmission.

# Results

We tested 84 parent-child dyads who participated in the "population-neuroscience study of the Tokyo TEEN Cohort (pn-TTC)," a longitudinal study exploring the neurobiological substrates of development during adolescence[63,64]. In the pn-TTC study, neuroimaging and non-imaging behavioural phenotypes were collected from children every 2 years from the age of 11, and from their primary parents (Figure 1a; see *Methods: Overview of the dataset*). Here, we used three brain datasets from the pn-TTC study: children at the ages of 11 and 13 years, and their primary parents. Parents' brains were scanned when their children were 11 years old. The basic demographic data are shown in Table 1.

**Table 1**: Demographic data. [a] Ages of parents when their children were 11 years old are shown.

| | N | Age[a] (mean ± s.t.d) | Sex (Male/Female) |
|---|---|---|---|
| Child age at 11 | | 11.59±0.66 | |
| Child age at 13 | 84 | 13.63±0.62 | 45/39 |
| Parent | | 43.35±3.95 | 3/81 |

We first defined the functional and structural whole-brain patterns for each individual (Figure 1a; see *Methods: Information extraction*). For fMRI, we used a functional atlas defining 268 regions of interest (ROIs) covering the entire brain[12,65]. The FC between these ROIs was estimated using Pearson's correlation coefficient, resulting in a 268 × 268 FC matrix for each subject. As the FC matrix is symmetrical, only the strictly lower triangular part of each matrix was kept, resulting in 35,778 (= 268 × 267 / 2) unique entries. We regressed potential confounds including total GMV and head motion. To further avoid the effects of motion artefacts, we employed a "scrubbing" procedure to identify and exclude any frames exhibiting excessive head motion[66]. We also obtained GMV for each ROI using T1w images, then averaged within each region. We used the same 268 ROIs as in the fMRI, resulting in a vector with a size of 268 for each subject.

To quantitatively evaluate the brain similarity of parent-child dyads, we proposed a framework to compare network-level similarity between parent-child dyads (Figure 1b; See *Methods: Similarity analysis* for details), inspired by a recently proposed approach for individual identification based on the brain[12]. To calculate the similarity of parent-child dyads,

128    we first calculated the correlations between a child's FC and/or GMV vector to all parents'

129    vectors including the child's own parent. We next assessed whether the similarity of the

130    parent-child dyad (child and his/her own parent) was larger than that of a stranger-child dyad

131    (child and another child's parent). We then calculated the winning rate of the similarity

132    between parent-child dyad, which was referred to as "accuracy", because it can be considered

133    as a "pairwise classification accuracy" when we randomly sampled a parent-child dyad and

134    another parent, then conduct classification (See *Methods: Similarity analysis* for details). We

135    repeated this procedure across all dyads and averaged these accuracies. Compared with

136    conventional individual identification methods, our proposed framework has more statistical

137    power, as described later. We performed 1,000-times bootstrapping to estimate 95%

138    confidence intervals of accuracy by randomly subsampling 90% of the subjects in each

139    iteration. To determine whether accuracy was achieved at above-chance levels, we used

140    1,000-times permutation testing to generate a null distribution by randomly shuffling the
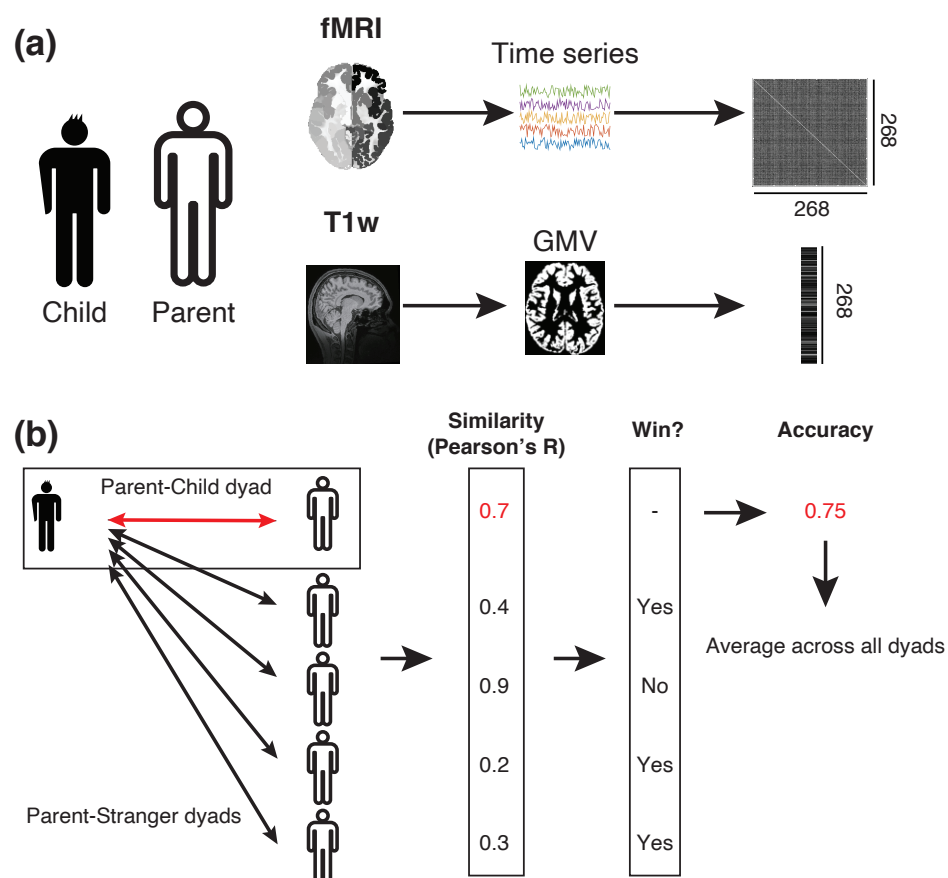
141    parent-child mapping.

142



143

144    **Figure 1**: **Analysis procedure of parent-child brain similarity**. (**a**) We employed a dataset obtained from the

145    "population-neuroscience study of the Tokyo TEEN Cohort (pn-TTC)" study, which consists of resting-state fMRI

146   and T1w images of parents and their children. To obtain a functional connectivity (FC) matrix, signals were

147   extracted from all subjects using resting-state fMRI data from 268 ROIs. The signals were then turned into an FC

148   matrix via covariance estimation. To obtain grey matter volume (GMV) vectors, T1w images were first segmented

149   into grey matter, white matter, and cerebrospinal fluid. Using the grey matter, GMV of each ROI was obtained by

150   averaging values within the ROI. We used the same 268 ROIs as in the FC. **(b)** For each parent-child dyad, we first

151   calculated the similarity of FC and/or GMV vectors based on their Pearson's correlation. We next calculated

152   similarities between the child and another child's parent. We then calculated whether the similarity of the

153   parent-child dyad is greater than that of stranger-child dyads. Finally, we calculated the winning rate of the

154   parent-child dyad ("accuracy"), and repeated this procedure across all parent-child dyads.

## Whole-brain analysis

156   We first assessed the similarity of parent-child dyads using whole-brain FC and GMV. When

157   we used a dataset of children at age 11, accuracies were 64.6% for FC (estimated via 1,000-

158   times bootstrapping; 95% CI = [62.5, 66.8]; P < 0.001, 1,000-times permutation test) and

159   70.3% for GMV (95% CI = [68.9, 71.8]; P < 0.001) (Figure 2a). When we used a dataset of

160   children at age 13, the accuracies were 66.7% for FC (95% CI = [64.5, 68.9]; P < 0.001) and

161   73.8% for GMV (95% CI = [72.1, 75.6]; P < 0.001) (Figure 2b). Thus, we provided the first strong

162   evidence that it is possible to identify parent-child dyads based on their functional and

163   structural brain information.

164   We next assessed the importance of information for performance of specific edges

165   for FC and regions for GMV, respectively (Figures 2c-2f). To quantify the extent to which

166   different edges and regions contribute to similarity, we derived two measures: the differential

167   power (DP) which calculates how characteristic edges and regions tend to be, and group

168   consistency ($\varphi$) which quantifies edges and regions that are highly consistent across all parent-

169   child pairs in a dataset[12] (see *Methods: Similarity analysis*). For visualisation purposes, we

170   show the structural locations of DP and $\varphi$ in the 99.75th and 90th percentile, for edges (FC)

171   and regions (GMV) respectively. For both FC and GMV, significant edges or regions tended to

172   be distributed across the entire brain. This pattern was stable across a range of thresholds

173   (Supplementary Figure 1). Note that, for visualisation purposes, we excluded the brainstem

174   from the figure for GMV because all regions in this area had extremely high $\varphi$ values, possibly

175   because of the much lower magnitudes of signals compared with the other regions

176   (Supplementary Figure 2).

177   Given that head motion confounds analyses of FC[66], we confirmed that qualitatively

178  similar results were obtained when we excluded parent-child dyads whose children's head

179  movements were in the top 25%, either at age 11 or 13, resulting in the inclusion of 41.25%

180  of the total sample (Supplementary Figure 3). We also confirmed that accuracy obtained by

181  the distribution of their frame-to-frame motion during fMRI scans[12] was not above chance

182  level (51.0% for age 11, 95% CI = [48.9, 53.0]; 48.7% for age at 13, 95% CI = [47.1, 50.1]). Thus,

183  it is unlikely that the identification power of FC was based on idiosyncratic patterns related to
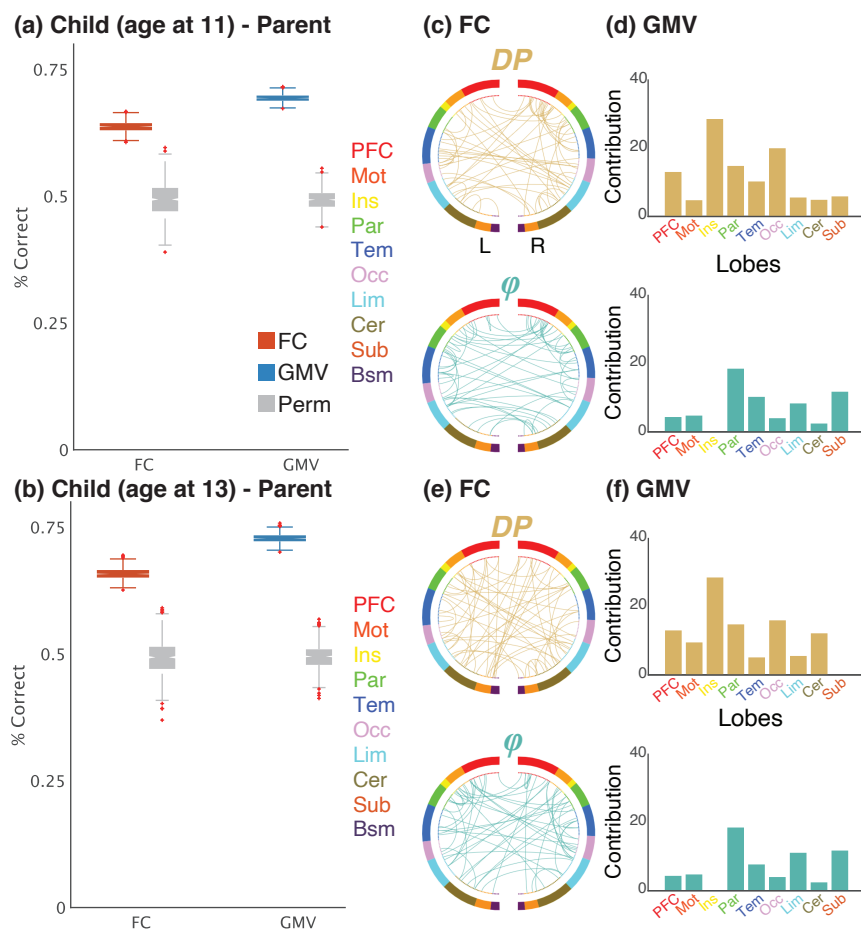
184  motion in the scanner.



185

**Figure 2**: **Successful identification of parent-child dyad based on their functional and structural brain information.** Box plots of parent-child identification accuracy and factors affecting accuracy for **(a)** children at age 11 and **(b)** at age 13 using whole-brain (268-node) for functional connectivity (FC: red box) and grey matter volume (GMV: blue box). Directly to the right of these boxes (grey box) are the results of the 1,000-times permutation testing. The bottom and top edges of the box indicate the 25th and 75th percentiles obtained via bootstrapping, respectively. The crosses denote outliers, and the whiskers extend to the most extreme data points not considered outliers. **(c–f)** Factors affecting identification accuracy. For FC, the top 99.75th percentile of differential power (DP: highly discriminative; yellow) edges and group consistency ($\varphi$: highly similar, or least helpful; green) edges are shown (circle plot; in which nodes are grouped according to anatomic location). For

195   GMV, the top 90th percentile ROIs of DP and $\varphi$ were calculated, then normalised by dividing the number of ROIs

196   in each anatomical group (bar plot). A legend indicating the approximate anatomical "lobe" is shown. PFC,

197   prefrontal; Mot, motor; Ins, insula; Par, parietal; Tem, temporal; Occ, occipital; Lim, limbic (including cingulate

198   cortex, amygdala, and hippocampus); Cer, cerebellum; Sub, subcortical (including thalamus and striatum); Bsm,

199   brainstem; L, left hemisphere; R, right hemisphere.

## Network-based similarity

201   We further investigated the contributions of specific networks to this similarity. We grouped

202   the whole regions into 10 sub-networks[67] (Figure 3a), and subsequently performed the same

203   analyses using only the edges and regions from a given network. Note that we calculated the

204   null distribution for each network via permutation testing, thus taking differences of the

205   number of edges/regions among networks into account.

206        For FC, medial frontal and frontoparietal networks led to high accuracies (Figure 3b).

207   In contrast, for GMV, default mode, subcortical, cerebellum and visual networks led to high

208   accuracy. Compared with FC, GMV achieved modestly higher accuracy than FC at age 11

209   (Figure 3c; paired sample t-test, $t(10) = -2.16$, $P = 0.056$, Hedge's $g = -0.72$) and significantly

210   higher accuracy at age 13 (Figure 3c; paired sample t-test, $t(10) = -3.10$, $P = 0.011$ , Hedge's $g$

211   $= -0.89$). To further assess the importance of each network, we next assessed performance

212   using between-network pairs of edges. We observed that edges between the medial frontal–

213   frontoparietal networks and medial frontal–motor networks resulted in higher accuracies

214   than the other between-network pairs (Supplementary Figure 4).

215        The results confirmed that our proposed method had greater statistical power than

216   conventional methods for individual identification (Supplementary Figure 5). Specifically, for

217   FC, six and five of 11 networks were significant at age 11 and 13, respectively, using the

218   conventional method, whereas nine and 10 networks, respectively, were significant in our

219   proposed method. For GMV, six and nine of 11 networks were significant at age 11 and 13,

220   respectively, using the conventional method, whereas all networks were significant using our

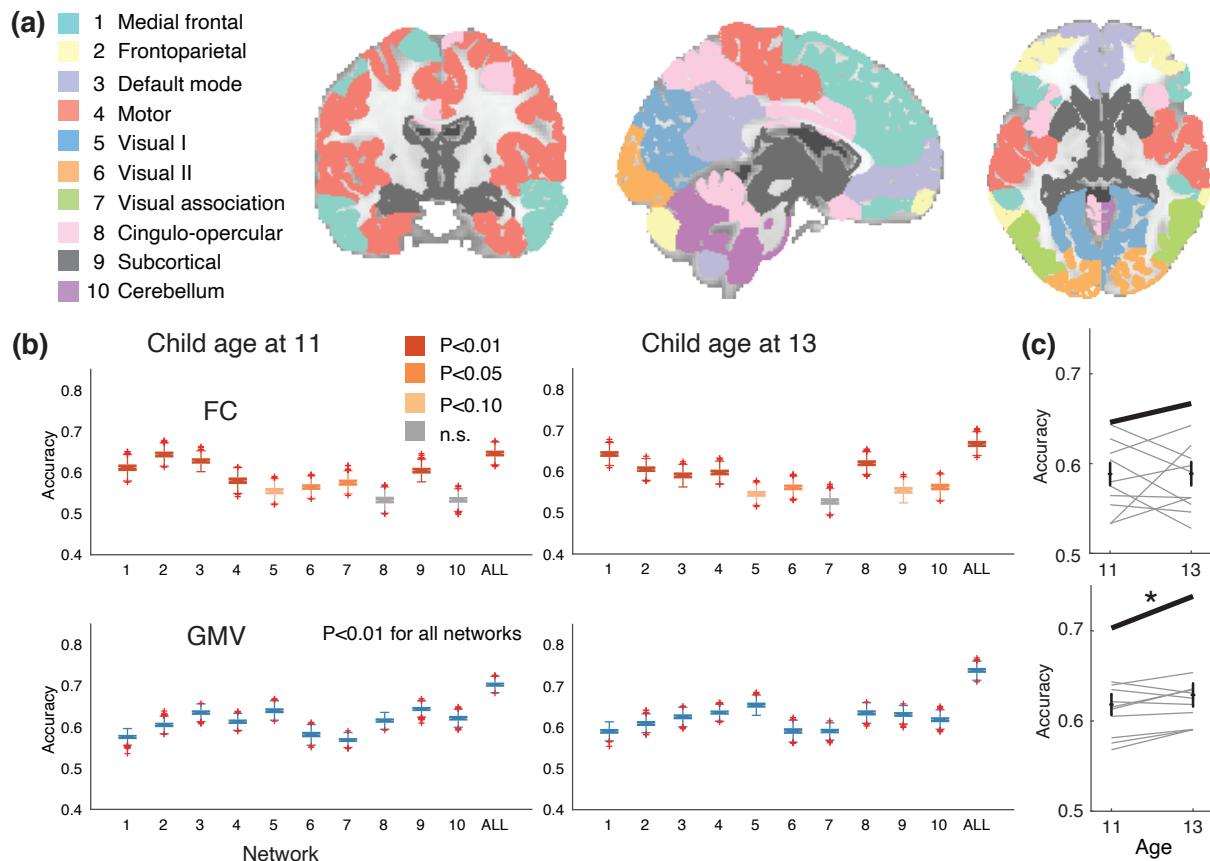221   proposed method.

9

**Figure 3**: **Network-based analyses demonstrated that almost all brain networks were highly similar between parents and their children**. (**a**) We utilised a 268-node functional atlas. Nodes were further grouped into the 10 functional networks. Network names are shown to the left. (**b**) Box plots of accuracies using within-network edges of FC analysis (top row; networks 1–10 and whole-brain (ALL); indicated below the x-axis of each graph) and within-network nodes of GMV (bottom row). The bottom and top edges of the box indicate the 25th and 75th percentiles, respectively. The crosses denote outliers, and the whiskers extend to the most extreme data points not considered outliers. (**c**) Comparison between accuracies of child age at 11 and 13 for FC (top row) and GMV (bottom row). Each scatter shows each network and line connected the same network. Bold lines indicate ALL. * paired sample t-test, $P < 0.05$, n.s. non-significant, uncorrected.

## Function and structure provide complementary information

Although FC and GMV revealed comparable performance in the above analyses, it remained unclear whether they contained similar information. This raises the following question: if parents and their children exhibit similar patterns of structural brain information, do they also exhibit similar patterns of functional brain information? Indeed, although functional and structural brain information is interrelated, they contain exclusive information that putatively

10

239  characterises distinct properties of individual differences[68]. To test this question, we
240  investigated the relationship between parent-child similarity defined by FC and that of GMV.
241  We found that the Pearson's correlation between the similarities defined by FC and GMV was
242  low: only two of 22 networks were significant (Supplementary Figure 6; P = 0.026 for visual
243  and P = 0.021 for whole-brain when we used data from children at age 13; the other networks
244  were not significant, P > 0.05, 1,000-times permutation test, uncorrected). Thus, although
245  both FC and GMV were similar between parent-child dyads, their characteristics were
246  dissimilar.

247         Given that FC and GMV appeared to contain independent information, we further
248  investigated whether they contained complementary information. To test this question, we
249  conducted the same analyses using both FC and GMV simultaneously by concatenating the
250  two vectors (hereafter referred to as "COMB"). COMB achieved the highest accuracies in more
251  than half of cases (15/22), compared with function (4/22) and structure (3/22) alone (Table
252  2). This number is significantly greater than chance (Supplementary Figure 7; P < 0.001, 1,000-
253  times permutation test). Overall, these results suggest that patterns of functional and
254  structural information contained complementary information in terms of parent-child brain
255  similarity.

256

**Table 2**: **COMB achieved higher accuracies compared with FC and GMV for many networks in children at age 11 and at age 13**. Means and 95% confidence intervals estimated via 1,000-times bootstrapping are shown. **Bold underlined** text indicates the best performance. MF, medial frontal; FP, frontoparietal; DMN, default mode network; Mot, motor; Vis I, visual I; Vis II, visual II; Vis A, visual association; Cing, cingulo-opercular; Sub, subcortical; Cer, cerebellum.

| Network | Age | FC | GMV | COMB |
|---|---|---|---|---|
| ALL | 11 | 64.60 [62.54,66.83] | 70.30 [68.86,71.75] | **70.64 [69.21,72.16]** |
| | 13 | 66.69 [64.50,68.86] | **73.82 [72.14,75.55]** | 73.57 [71.89,75.30] |
| 1. MF | 11 | **61.14 [58.83,63.66]** | 57.56 [56.02,58.94] | 58.32 [56.77,59.66] |
| | 13 | **64.26 [62.20,66.36]** | 59.02 [57.06,60.70] | 59.14 [57.14,60.92] |
| 2. FP | 11 | **64.35 [62.40,66.52]** | 60.52 [59.01,62.20] | 61.90 [60.38,63.55] |
| | 13 | 60.57 [58.61,62.49] | 60.94 [59.35,62.65] | **61.79 [60.25,63.46]** |
| 3. DMN | 11 | 62.77 [61.06,64.65] | 63.49 [61.93,64.94] | **63.66 [62.04,65.21]** |
| | 13 | 59.07 [57.03,61.03] | 62.53 [60.77,64.23] | **62.84 [61.05,64.50]** |
| 4. Mot | 11 | 57.95 [55.60,60.29] | 61.30 [59.80,62.85] | **62.27 [60.70,63.82]** |
| | 13 | 59.78 [57.89,61.77] | 63.56 [61.95,65.14] | **64.27 [62.63,65.98]** |
| 5. Vis I | 11 | 55.42 [53.19,57.59] | 63.98 [62.40,65.59] | **64.91 [63.23,66.58]** |
| | 13 | 54.60 [52.61,56.77] | 65.37 [63.60,67.21] | **65.98 [64.20,67.77]** |
| 6. Vis II | 11 | 56.44 [54.41,58.61] | 58.14 [56.20,60.04] | **58.95 [57.14,60.81]** |
| | 13 | 56.20 [54.14,58.25] | 59.07 [56.95,61.03] | **60.33 [58.22,62.32]** |
| 7. Vis A | 11 | **57.52 [55.35,59.86]** | 56.81 [55.51,58.02] | 57.13 [55.84,58.31] |
| | 13 | 52.78 [50.50,55.06] | **59.05 [57.28,60.56]** | 58.92 [57.28,60.41] |
| 8. Cing | 11 | 53.28 [51.08,55.66] | **61.54 [59.89,62.99]** | 61.53 [59.91,62.94] |
| | 13 | 62.04 [59.93,64.34] | 63.48 [61.51,65.17] | **63.71 [61.68,65.46]** |
| 9. Sub | 11 | 60.43 [58.52,62.59] | 64.34 [62.67,65.95] | **64.66 [62.97,66.23]** |
| | 13 | 55.45 [53.23,57.62] | 63.08 [61.41,64.65] | **63.61 [62.00,65.19]** |
| 10. Cer | 11 | 53.32 [51.23,55.37] | 62.13 [60.38,63.73] | **62.86 [61.24,64.54]** |
| | 13 | 56.24 [53.87,58.68] | 61.83 [59.91,63.71] | **62.50 [60.67,64.34]** |
| # best | | 4 | 3 | 15 |

## Effects of demographic factors on the brain similarity

12

264        The results described above indicated strong intergenerational transmission effects
265    on the brain from parents to their children. However, it was still unclear whether all parent-
266    child dyads were equally similar. Therefore, we then investigated which factors influence brain
267    similarity. Here, we focused on fundamental demographic factors: age and sex.

268        We found that accuracies at age 11 were significantly lower than those at age 13 for
269    GMV (Figure 3c bottom; paired sample t-test, $t(10) = -2.39$, $P = 0.038$ , Hedge's $g = -0.25$),
270    whereas they were no different for FC (Figure 3c top; paired sample t-test, $t(10) = -0.03$, $P = $
271    $0.97$, Hedge's $g = -0.01$).

272        We then divided children into males and females (Figure 4). The results confirmed
273    that both male and female children exhibited significant accuracies for almost all networks, as
274    in the previous analyses (Figure 4a). When we compared males and females (Figure 4b), the
275    accuracies of female children were significantly higher than those of male children for FC, at
276    both age 11 (paired sample t-test, $t(10) = -2.34$ , $P = 0.04$, Hedge's $g = -0.88$) and age 13
277    (paired sample t-test, $t(10) = -3.80$ , $P = 0.003$ , Hedge's $g = -1.21$). Female children also
278    exhibited higher accuracy than male children for GMV at age 13 (paired sample t-test, $t(10) = $
279    $-2.47$ , $P = 0.03$, Hedge's $g = -0.83$), but not at age 11 (paired sample t-test, $t(10) = -0.25$, $P = $
280    $0.81$ , Hedge's $g = 0.07$).

281        When we compared accuracies at age 11 and age 13 for male and female children
282    separately (Figure 4c), female children at age 13 had significantly greater accuracy than those
283    at age 11 for GMV (paired sample t-test, $t(10) = -3.75$, $P = 0.004$, Hedge's $g = -0.76$). All other
284    comparisons were not significant: male, FC (paired sample t-test, $t(10) = 0.37$, $P = 0.72$,
285    Hedge's $g = 0.13$); male, GMV (paired sample t-test, $t(10) = 2.05$ , $P = 0.068$, Hedge's $g = 0.23$);
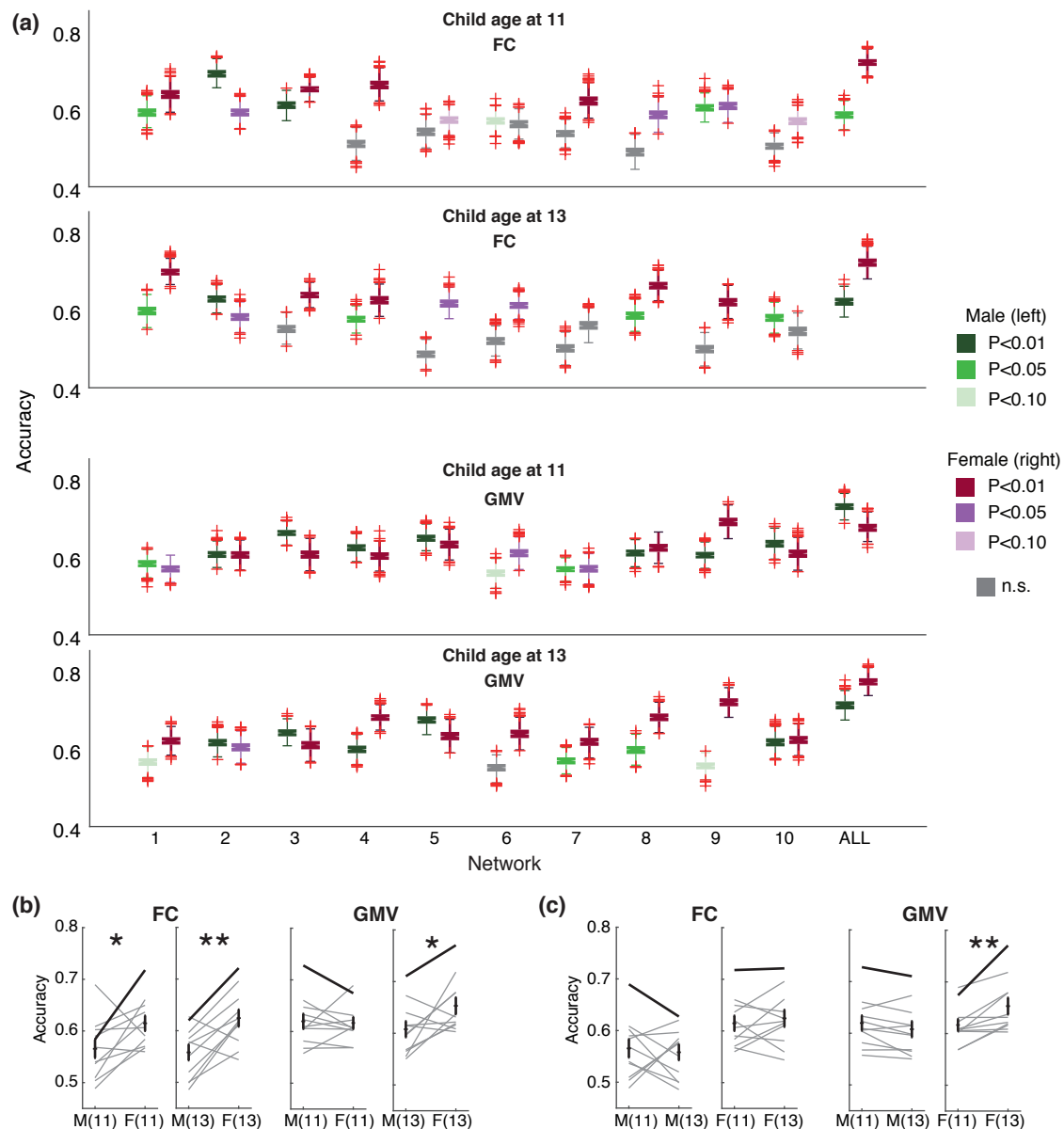286    female, FC (paired sample t-test, $t(10) = -0.73$ , $P = 0.48$, Hedge's $g = -0.18$)

**Figure 4: Male and female children show different trends of brain similarity across development.** (a) Accuracies split by children's sex for FC and GMV. For each network, accuracies for males (left boxes) and females (right boxes) are shown. (b) Comparison between males and females. (c) Comparison between children age at 11 and 13. Each scatter shows each network and line connected the same network. Bold lines indicate ALL. M(11), males at age 11; F(11), females at age 11; M(13), males at age 13; M(13), males at age 13; * Paired sample t-test, P < 0.05; ** P < 0.01. n.s. non-significant, uncorrected.

## Effects of behavioural phenotypes on brain similarity

Finally, we examined whether behavioural phenotypes have effects on the brain similarity of parent-child dyads. Here, we used two important behavioural phenotypes for adolescents: hormone level and questionnaire-based developmental score (Figure 5; see

14

298  *Methods: Testosterone and Child Behavior Checklist*). We used COMB for this analysis as brain

299  information.

300  We examined testosterone as a hormone level, because it is known that the

301  pubertal period is a sensitive period for testosterone-dependent organisation of the brain[69].

302  We found that children with high testosterone exhibited significantly higher accuracy

303  compared with children with low testosterone at age 11 (paired sample t-test, t(10) = −2.91,

304  P = 0.016, Hedge's g = −1.03) but not at age 13 (paired sample t-test, t(10) = −0.60, P = 0.56,

305  Hedge's g = −0.22).

306  We next investigated the effects of a questionnaire-based development score (Child

307  Behavior Checklist: CBCL)[70]. The CBCL is a parental-report assessment used to screen for

308  emotional, behavioural, and social problems, and to predict psychiatric illnesses[71]. We found

309  that children with high CBCL had significantly higher accuracy compared with children with

310  low CBCL at age 11 (paired sample t-test, t(10) = −2.81, P = 0.018 , Hedge's g = −1.05) but not

311  at age 13 (paired sample t-test, t(10) = −0.99, P = 0.34, Hedge's g =−0.33).
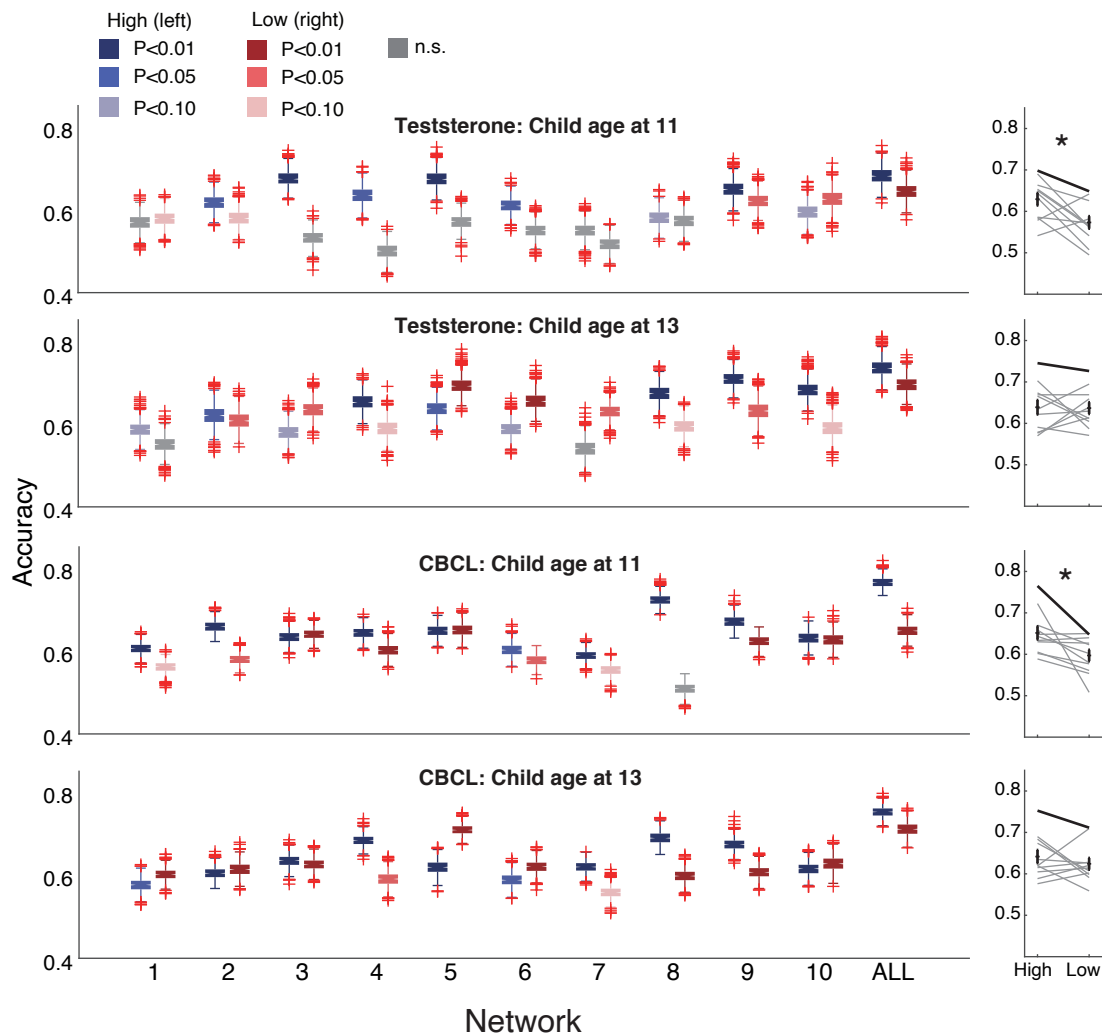
312

**Figure 5: Behavioural phenotypes have effects on brain similarity**. Accuracies split by testosterone and CBCL. Left panels: Boxplots of accuracies split by scores of behavioural phenotypes (left: upper-half children; right: lower-half children). Right panels: Comparisons between upper- (left) and lower-half (right) children. Each scatter shows each network and line connected the same network. Bold lines indicate ALL. * Paired sample t-test, P < 0.05. n.s. non-significant, uncorrected.

# Discussion

The present study revealed that patterns of functional and structural brain information are preserved over a generation. Although the effects of the intergenerational transmission have been investigated in various research fields, including developmental psychology, educational psychology, and economics, no study has comprehensively and quantitatively investigated the neurobiological substrates of intergenerational transmission. The current results revealed that, despite substantial differences between parents and their children, their brains are sufficiently similar that we can identify parent-child dyads based on information about their brains. We employed a rigorous statistical framework and an unusually large functional and structural neuroimaging dataset of parent-child dyads with rich behavioural phenotypes (N = 84 parent-child dyads)[63,64]. Although both functional and structural brain information has comparable levels of accuracy, their characteristics were different but complementary. Demographic factors and behavioural phenotypes also have large effects on brain similarity. Taken together, our results provide a detailed picture of whether, to what extent, and how brains of parent-child dyads are similar.

Previous studies have reported that brain information is heritable. Several genome-wide association studies (GWAS) have been conducted to identify genetic risk variants for GMV[25,44,50–56] and FC[25,26]. Although heritable regions or edges have been successfully identified, most studies have been insufficiently powered because GWAS require a large sample size (although some studies used multivariate approaches to increase statistical power[26,58]). In addition, these studies typically did not consider the effects of demographic and behavioural phenotypes. In addition to GWAS, both twin and family-based studies have reported that GMV[45–49,57] and FC[27–43] are heritable. These studies typically achieve larger effect sizes than GWAS studies with smaller sample sizes, although the possibility of inflated effect sizes due to shared environments is a concern. These studies also typically ignore demographic and behavioural phenotypes by treating them as covariates. Importantly, none of the previous studies described here directly investigated the effects of intergenerational transmission from parents to children.

In recent years, some studies directly investigated intergenerational transmission of brain information using parent-child dyads. Although extended pedigree studies with sufficient sample sizes could answer such a question, it is logistically more difficult to recruit participants for pedigree studies than for studies with a parent-child design. Thus, parent-child

17

353 design studies play a complementary role in the investigation of intergenerational

354 transmission. For example, some studies found that, during specific tasks, brain activity of

355 parent-child dyads was synchronised[60,61]. Other, more relevant studies to the current studies

356 reported that patterns of FC [59] and GMV [62] were similar between parent-child dyads. However,

357 these studies did not quantitatively and comprehensively investigate the effects of different

358 brain networks, and did not compare FC and GMV. It is also unclear which factors affect brain

359 similarities, including age, sex, hormonal level, and behavioural traits (although Yamagata et

360 al. investigated the effects of sex on GMV-based similarity using ROI-based analyses [62]). This

361 is partly because investigating such questions require a large neuroimaging dataset of parent-

362 child dyads with rich behavioural phenotypes. Overall, the present study is the first to

363 investigate whether, to what extent, and how brains of parent-child dyads are similar.

364 For both function and structure, the brain regions that contributed to similarity

365 tended to be broadly distributed across the entire brain when we used whole-brain

366 information (Figure 2c–2f), as in previous FC-based individual identification studies[12,67].

367 Although this tendency was retained when we only used the edges or regions within sub-

368 networks, we observed slightly different contrasts between functional and structural

369 information (Figure 3b and Table 2). Specifically, for function, the medial frontal and

370 frontoparietal areas, which are known to be involved in networks related to higher cognitive

371 function, revealed higher accuracies than structural information. In contrast, for structure,

372 visual, subcortical, and cerebellum networks exhibited higher accuracies than function. This

373 contrast is interesting because the prefrontal cortex is one of the last regions of the brain to

374 reach maturation, exhibiting development until approximately 25 years of age, whereas

375 subcortical regions reach maturation earlier[72]. Note that, for structural brain information, only

376 a small number of studies using GMV are comparable to the current study[73,74], and none of

377 them investigated each network's contribution in detail.

378 We confirmed that our results were not solely driven by structural or functional

379 similarity alone. The neural similarity between FC and GMV exhibited a weak correlation

380 (Supplementary Figure 6). In addition, combining FC and GMV led to the highest accuracy for

381 many brain regions (Table 1). These results indicate that FC and GMV are distinct and contain

382 complementary information. Previous studies reported that function and structure contain

383 similar information, but also distinct information[68]. One study reported that information

384 obtained from function and structure contain complementary information for the

385 identification of siblings, but did not investigate the contributions of distinct anatomical brain

18

386    locations[75]. The current results are not only consistent with those of previous studies but also
387    demonstrated qualitative differences between function and structure by exhaustively
388    investigating the contributions of each distinct anatomical brain location. It is noteworthy that
389    GMV was able to obtain similar accuracy, even with short scans that are routinely acquired as
390    initial scans in MRI protocols.

391    We also found that several demographic and behavioural factors had effects on the
392    brain similarity of parent-child dyads. First, we found that age had an effect on accuracies of
393    GMV, but not FC. It is known that both FC and GMV change through adolescence[76,77]; thus,
394    this difference suggests that the functional and structural development of the brain are not
395    qualitatively equal, at least from the perspective of parent-child similarity. Second, when we
396    split children into males and females, we found age effects on the brains of female children,
397    both for FC and GMV. This finding suggests that the developmental trajectory of the brain
398    qualitatively differs between females and males. In addition, female children were more
399    similar to their parents than male children, particularly at age 13. This finding is intriguing
400    because previous studies also reported that female children are more similar to their mothers
401    both behaviourally[78] and neurally[62]. Third, testosterone affected brain similarity in parent-
402    child dyads. Interestingly, children with high levels of testosterone exhibited greater similarity
403    than other children, despite female children having greater accuracy than male children. Note
404    that there were no significant differences in levels of testosterone between males and females
405    both at age 11 (two-sample t-test, $t(49) = -0.64$, $P = 0.53$, Hedge's $g = -0.19$) and 13 (two-
406    sample t-test, $t(44) = 0.81$, $P = 0.42$, Hedge's $g = 0.25$). It is known that levels of testosterone
407    increase through adolescence, especially in male children[79]. Thus, different results may have
408    been obtained if older children were tested. Fourth, questionnaire-based development scores
409    had effects on similarity. Children with higher developmental problem scores were more
410    similar to their parents than other children. Although this result is somewhat counterintuitive,
411    it suggests that similarity of the brain does not merely represent behavioural maturity
412    assessed by questionnaire. Overall, the current results provide the first detailed picture of the
413    signature of intergenerational transmission in the brain.

414    Recent developments in cognitive neuroscience have made it possible to investigate
415    individual differences, an issue that has not been deeply investigated because of the absence
416    of adequate datasets, analytical techniques, and computational resources. The current results
417    shed light on the importance of investigating family-level differences, in addition to individual-
418    level differences. Families are not a neutral environment for identity development, but deeply

19

419   affect individuals from adolescence, strongly influencing the development of a person's
420   identity[80]. Given that the current results revealed that parental brains are similar to the brains
421   of their children, we propose that future studies should investigate the relationships between
422   family-level behavioural indices and family-level brain information to enable more reliable
423   predictions of children's behaviour and development. We believe our dataset will help to
424   extend research in this direction[64].

425       The current findings indicate several potentially interesting questions for future
426   research. The first and perhaps most important question is whether parent-child brain
427   similarity changes across children's development. Recent studies proposed a brain-based
428   quantitative approach for investigating the trajectory of development[81,82]. Although the
429   current study revealed that children at age 11 and age 13 are different, it may be valuable to
430   investigate whether the trajectory of the parent-child brain similarity affects the various risks
431   faced by adolescents, including psychiatric disorders and criminal behaviour, using much
432   longer-term longitudinal datasets. Second, insights may be gained by using genetic
433   information to confirm the extent to which genetic factors contribute to neural similarity. We
434   examined biological parent-child relationships in the current study. Thus, it may be valuable
435   to test whether non-biological parents and children show the same level of brain similarity.
436   Third, we used GMV as a structural brain measurement because a number of previous studies
437   investigated the relationship between GMV and various traits. However, the human brain also
438   exhibits individual differences in white matter microstructure. Diffusion tensor imaging
439   provides measures of white matter integrity in the brain, and can provide useful data, but, like
440   GMV, produces different information to FC[83]. Indeed, previous studies have shown that
441   thickness correlations partially reflect underlying fibre connections but contain exclusive
442   information[84]. Future studies should use other types of structural information, such as
443   structural connectivity obtained by diffusion tensor imaging. Fourth, because our dataset
444   mostly consisted of mothers (81 mothers among 84 parents), it may be valuable to test
445   whether we can also identify children' brains from fathers. Although we confirmed that we
446   were able to successfully conduct analyses both male and female children, future studies
447   should investigate the effects of parents' sex on performance.

448       In the present study, we sought to address a critical question in social science:
449   whether, to what extent, and how parents and children are similar. Our analytical framework
450   and the richness of our dataset made it possible to ask the question from the neurobiological
451   perspective. The results revealed that parents' and their children's brains exhibit a high degree

452    of similarity, and that various factors, including age, sex, hormones, and development score

453    have effects on similarity. These results provide a comprehensive picture of the

454    neurobiological substrates of parent-child similarity, and show the usability of our dataset for

455    investigating the neurobiological substrates of intergenerational transmission.

## Acknowledgments

## Author Contributions

468    N.O., S.A., N.Y., K.M., D.K., S. Kawakami, K.S., S. Koike, K.E., S.Y., A.N., K.K., and S.C.T. recruited

469    participants for the study and collected their behavioural and imaging data. N.O. inspected

470    imaging data. N.Y. provided codes for preprocessing resting state fMRI data. S. Koike, and K.K.,

471    interpreted the results and provided technical advice. S.C.T. supervised the study. Y.T.

472    conceptualised the study, conducted the analysis, visualised the data, and wrote the

473    manuscript. All authors reviewed the manuscript.

## Data and code availability statement

475    The data that support the findings of the current study may be available from the

476    corresponding author upon reasonable request (http://value.umin.jp/data-resource.html).

477    The code supporting the findings of this study will be published after acceptance.

# Methods

## Overview of the dataset

The Tokyo TEEN Cohort (TTC) study, which was launched in 2012, is a large-scale longitudinal general population-based survey to elucidate puberty development during adolescence, particularly the acquisition processes of self-regulation and willingness to face challenges, by focusing on the interaction between biological, psychological, and social factors[63,64]. This study was conducted as part of the population-neuroscience component of the TTC (pn-TTC) study, in which 301 early adolescents were recruited from the general population. Subjects of the pn-TTC study were subsampled from a larger subject group of the TTC study, and it was confirmed that the pn-TTC subsample was representative of the TTC study population. Written informed consent was obtained from each subject and the subject's primary parent before participation. All protocols were approved by the research ethics committees of the Graduate School of Medicine and Faculty of Medicine at the University of Tokyo, Tokyo Metropolitan Institute of Medical Science, and the Graduate University for Advanced Studies. All research was performed in accordance with relevant guidelines/regulations. The detailed methods for subject recruitment are described elsewhere[63,64]. The dataset is publicly shared upon request (http://value.umin.jp/data-resource.html).

We excluded subjects who exhibited anomalies in fMRI or T1w images. We also excluded parents who did not have either fMRI or T1w images, and children who did not have either fMRI or T1w images at age 11 and age 13. After this screening process, 84 dyads were included in the final analysis (39 female children; 81 mothers; age = 11.59 ± 0.66 for children at age 11, 13.63 ± 0.62 for children at age 13, and 43.35 ± 0.62 for parents, mean ± s.t.d).

## MRI parameters

Subjects were instructed to lie supine on the bed of the MRI scanner. MRI scanning was performed on a Philips Achieva 3T system (Philips Medical Systems, Best, The Netherlands) using an eight-channel receiver head coil. Each subject underwent resting-state fMRI and T1-weighted (T1w) three-dimensional magnetisation-prepared rapid gradient echo (3D-MPRAGE) sequences.

Sagittal T1w images were acquired using the 3D-MPRAGE sequence with the

507  following parameters: repetition time (TR) = 7.0 ms, echo time (TE) = 3.2 ms, minimum

508  inversion time = 875.8 ms, flip angle = 9°, matrix = 256 × 256, field of view (FOV) = 256 mm ×

509  240 mm × 200 mm, voxel size = 1 mm × 1 mm × 1 mm, slice thickness = 1 mm, number of

510  slices = 200. The acquisition time was approximately 10 min 42 sec.

511  Resting-state fMRI images were acquired using a gradient-echo echo-planar imaging

512  (EPI) sequence with the following parameters: TR / TE, 2500 ms / 30 ms; flip angle, 80°; matrix,

513  64 × 64; FOV, 212 mm × 199 mm × 159 mm; voxel size, 3.31 mm × 3.31 mm; slice thickness,

514  3.20 mm; slice gap, 0.8 mm. Each brain volume consisted of 40 axial slices and each functional

515  run contained 250 image volumes preceded by four dummy volumes, resulting in a total scan

516  time of 10 min 40 sec. Subjects were instructed to stay awake, to keep their minds as clear as

517  possible, and to keep their eyes on a fixation point at the centre of the screen through a mirror

518  during scanning.

519  **Information extraction**

520  We used Statistical Parametric Mapping 8 (SPM8: Wellcome Department of Cognitive

521  Neurology, http:/ /www.fil.ion.ucl.ac.uk/spm/software/) in MATLAB (MathWorks, Natick,

522  Massachusetts) for preprocessing and statistical analyses.

523  *Preprocessing of* structural *MRI:* T1w images were segmented into three tissue

524  classes (grey matter [GM], white matter [WM], and cerebrospinal fluid [CSF]) using a

525  segmentation approach implemented in SPM8. The segmented images (only GM) were then

526  normalised into standardised Montreal Neurological Institute (MNI) space by applying a

527  deformation field in SPM8. The GMV of each ROI was extracted and averaged within that ROI.

528  We used a functional atlas defining 268 ROIs that cover the entire brain (functional atlas from

529  Finn et al.[12], which used the method developed by Shen et al.[65]) (this atlas can be downloaded

530  from https://www.nitrc.org/frs/?group_id=51), enabling us to obtain a vector with a size of

531  268 for each subject. Note that, although an alternative method for inter-subject registration

532  called Diffeomorphic Anatomical Registration Exponentiated Lie algebra (DARTEL) exists, we

533  did not employ it because our goal was not to conduct comparisons at the group-level. Future

534  studies should investigate whether employing another segmentation and normalisation

535  method can improve accuracy.

536  *Preprocessing of resting-state fMRI:* Preprocessing of resting-state fMRI included

537  slice-timing correction, realignment, co-registration, normalisation to MNI space, and spatial

23

538    smoothing with an isotropic Gaussian kernel of 6 mm full-width at half-maximum. To avoid

539    the effects of head motion artefacts, we calculated framewise displacement (FD). FD is

540    defined as the mean relative displacement between two consecutive volumes for each of the

541    six motion parameters. We conducted a "scrubbing" procedure by removing volumes with FD

542    > 0.5 mm, along with the previous volume and two subsequent volumes, as proposed by

543    Power et al.[66] The average grey matter time-course for each ROI was calculated, then

544    temporally filtered using a first-order Butterworth filter with a pass band between 0.01 Hz and

545    0.08 Hz. The time-course of each ROI was linearly regressed by the temporal fluctuations in

546    white matter, cerebrospinal fluid, and the entire brain, as well as six head motion parameters.

547    The time-course of white matter and cerebrospinal fluid were filtered using a first-order

548    Butterworth filter with a pass band between 0.01 Hz and 0.08 Hz, and a white matter mask

549    was eroded by one voxel to consider a partial volume effect. All parameters were determined

550    in accord with a previous study[19]. For each subject, an FC matrix between all ROIs was then

551    calculated by evaluating pair-wise temporal Pearson's correlations of blood-oxygenation level

552    dependent time courses, based only on the remaining images after the scrubbing step above.

553    We used the same 268 ROIs that were used for GMV. Because FC matrices are symmetrical,

554    values on only one side of the diagonal were kept, resulting in 35,778 unique edges (268 ×

555    267/2). We then regressed the motion and total grey matter volume and mean FD out from

556    data matrices.

557          *Motion index:* In addition to resting-state fMRI and structural MRI information, we

558    performed the same analyses using motion estimates during resting-state fMRI to investigate

559    the effects of motion artefacts[12]. We first specified 20 bins to span {0:0.05:1} to calculate

560    discrete motion distribution vectors for each parent and child based on FD over an entire scan.

561    These motion distribution vectors were then used in the same way as the FC or GMV vectors.

562    **Similarity analysis**

563    We modified a connectome fingerprinting approach by Fin et al[12]. They used two datasets

564    consisting of the same individual but different task sessions, called "source" and "target"

565    dataset. They correlated the connectivity vector from one participant in the source dataset to

566    the vectors of all participants in the target dataset and identified the maximum correlation. If

567    the two vectors showing the strongest correlations came from the same individual, the

568    resulting binary accuracy was 100%, whereas binary accuracy was 0% otherwise. Although

569    these studies successfully identified brain networks that contributed to the individual

570 identification, their method treats second-ranked and worst-ranked cases as equally failed
571 cases, thus discarding some information that might be useful for improving the statistical
572 power. In addition, the chance rate depends on the number of samples, thus making the
573 interpretation difficult, especially comparing different datasets with different sample sizes. To
574 overcome these issues, we modified the method as follows. We confirmed that the proposed
575 method is more sensitive than conventional methods (Supplementary Figure 5) and the
576 chance rate was always 50%, irrespective of the sample size.

577 For each parent-child dyad, we first calculated the similarity of their FC and/or GMV
578 patterns based on their Pearson's correlation. We next assessed whether the similarity of the
579 parent-child dyad (child and their own parent) was larger than a stranger-child dyad (child and
580 another child's parent). We then calculated the winning rate of the similarity between parent-
581 child dyad, denoted as "accuracy". We repeated this procedure across all children and
582 averaged accuracies.

583 Intuitively, the obtained statistics can be considered as a "pairwise classification
584 accuracy" calculated by the following procedure:
585 1. Select a child randomly from all children in the sample.
586 2. Select two parents, including the child's own parent and a randomly selected parent in the
587 sample.
588 3. If the Pearson's correlation coefficient between parent-child dyad is higher than that of
589 stranger-child dyad, the result is recorded as a correct parent-child identification.
590 4. In contrast, if the Pearson's correlation coefficient between parent-child dyad is smaller
591 than that of stranger-child dyad, it is recorded as a failed identification.
592 5. Repeat this procedure and calculate accuracy across repetition.
593 By increasing the number of repetitions, this approach converges to the accuracy
594 obtained by the main analysis. The chance rate of this approach is always 50%.

595 We performed 1,000-times bootstrapping to estimate the 95% confidence interval
596 of accuracy, by randomly subsampling 90% of the subjects in each iteration. To determine
597 whether accuracy was achieved at above-chance levels, we used 1,000-times permutation
598 testing to generate a null distribution by randomly shuffling the parent-child mapping.

599 To determine the role of specific edges/regions in the performance, we quantified
600 highly unique and highly consistent edges/regions using a differential power (DP) measure
601 and a group consistency measure ( $\phi$ ) described in detail elsewhere[12]. DP provides an

602 estimate, for each given edge/region, of the likelihood that within parent-child dyad similarity

603 (between a parent and their parent) is higher than stranger-child similarity (between a parent

604 and another parent's child). Specifically, we computed the edge/region product vector ($\varphi_i$)

605 from two sets of FC/GMV vectors $[X_i^{Child}]$, $[X_i^{Parent}]$,

609
$$\varphi_i(f) = X_i^{Child}(f) * X_i^{Parent}(f), f = 1, 2, \dots, M$$

606 where $i$ indexes dyad, $f$ indexes edge/region, and $M$ is the total number of edges/regions in

607 the entire FC/GMV vector. We can calculate $\varphi_i$ between vectors of a child and another child's

608 parent

610
$$\varphi_{ij}(f) = X_i^{Child}(f) * X_j^{Parent}(f), i \neq j$$

611 To compute the DP for all the dyads in a given dataset, we calculate an empirical

612 probability

613
$$P_i(f) = \frac{P\left(\left|\varphi_{ji}(f) > \varphi_{ii}(f)\right| + \left|\varphi_{ij}(f) > \varphi_{ii}(f)\right|\right)}{2(N)}, N = number\ of\ dyads$$

614 A low $P_i(f)$ indicates a more discriminative edge/region. We can finally calculate

615 DP of an edge/region across all children in a sample:

616
$$DP(e) = \sum_i \{-\ln(P_i(e))\}$$

617 If the parent-child dyad product was higher than the stranger-child product across

618 all children in a sample, this corresponds to a high DP value, and the edge/region is helpful.

619 The group consistency measure, $\varphi$ is simply the mean of $\varphi_i$ for a given edge/region

620 across all children. Edges/regions with high $\varphi$ values are therefore high across all pairs of

621 children and parents, and thus are not helpful.

622 For the analyses in Figure 2, we used whole-brain FC or GMV. For the analyses of

623 data shown in Figure 3, we split the whole brain into 10 sub-networks and conducted the

624 same analyses using FC or GMV within each sub-network. The definition of sub-networks was

625 obtained from Horien et al.[67].

626 **Testosterone and Child Behavior Checklist**

627 We investigated the effects of testosterone and Child Behavior Checklist (CBCL) scores on the

628 brain similarity of parent-child dyads. The detailed methods for data collection are described

629 elsewhere[63,64]. In the main analyses, we excluded dyads if either parent or child did not have
630 a score. We also excluded children who had an extremely high testosterone measurement
631 (more than mean + 1.5 s.t.d. Mean values of excluded children were 41.65 pg/mL [N=4] and
632 92.63 pg/mL [N=7] for children at age 11 and 13, respectively). After exclusion, the number of
633 dyads was 51 for testosterone at age 11 (4.01 ± 3.63 pg/mL, mean ± s.t.d), and 46 for
634 testosterone at age 13 (15.96 ± 17.83 pg/mL, mean ± s.t.d), 82 for CBCL at age 13 (6.55 ± 6.16,
635 mean ± s.t.d). There was no exclusion for CBCL age at 11 (10.48 ± 9.10, mean ± s.t.d).

636 1. *Testosterone:* The adolescents collected their salivary samples at home early in the
637 morning. In advance, both the adolescents and their primary parents were informed of
638 how to collect the adolescents' saliva using sample tubes. The adolescents tried it under
639 the guidance of the survey staff for practice. They were instructed not to collect the saliva
640 within a week after a tooth extraction or immediately after dental treatment to avoid
641 contamination with blood. They were also asked not to eat food after brushing their teeth
642 on the night before the saliva collection. They were instructed to rinse their mouth soon
643 after getting up and to make sure they were at their normal body temperature, and not to
644 have breakfast and not to brush teeth before the collection. Furthermore, they were asked
645 to wait for 20 min after the rinse and then to collect 4.5 ml of their saliva by passive drool
646 in sterilized tubes (1.5 ml/tube * 3 tubes) made of polypropylene (Nalgene[TM] General
647 Long-Term Storage Cryogenic Tubes, Thermo Fisher SCIENTIFIC, U.S.A.) within 60 min.
648 Salivary samples were collected in only one day, since high correlation among morning
649 salivary testosterone levels across days in adolescents was reported[85]. Salivary samples
650 were kept in household refrigerator freezers, delivered frozen to our laboratory, where the
651 weights were measured and tubes stored at minus 80 degrees C until the testosterone
652 levels were measured. The concentration of salivary testosterone was measured once by
653 liquid chromatography- tandem mass spectrometry (LC–MS/MS), which has become the
654 current standard[86]. All testosterone measurements were then square-eroot transformed
655 to better approximate a normal distribution prior to quantitative analyses.

656 2. *CBCL:* CBCL is a parental-report questionnaire used to screen children for behavioural
657 problems: there are 20 competence items and 120 items on behavioural and emotional
658 problems. The CBCL includes the following eight empirically-based syndrome scales: 1)
659 Aggressive Behavior, 2) Anxious/Depressed, 3) Attention Problems, 4) Rule-Breaking
660 Behavior, 5) Somatic Complaints, 6) Social Problems, 7) Thought Problems, and 8)
661 Withdrawn/Depressed, as well as summary scores reflecting "Internalization" and
662 "Externalization." We used the average scores of "Internalization" and "Externalization" in

27

663     the main results.

664

# References

1. de Graaf, P. M. & Kalmijn, M. Trends in the Intergenerational Transmission of Cultural and Economic Status. *Acta Sociol.* **44**, 51–66 (2001).

2. Deary, I. J., Spinath, F. M. & Bates, T. C. Genetics of intelligence. *Eur. J. Hum. Genet.* **14**, 690–700 (2006).

3. Grønhøj, A. & Thøgersen, J. Like father, like son? Intergenerational transmission of values, attitudes, and behaviours in the environmental domain. *J. Environ. Psychol.* **29**, 414–421 (2009).

4. Kalmuss, D. The intergenerational transmission of marital aggression. *J. Marriage Fam.* 11–19 (1984).

5. Corak, M. Income inequality, equality of opportunity, and intergenerational mobility. *J. Econ. Perspect.* **27**, 79–102 (2013).

6. Demirkan, A. *et al.* Genetic risk profiles for depression and anxiety in adult and elderly cohorts. *Mol. Psychiatry* **16**, 773–783 (2011).

7. Miller, R. B. & Glass, J. Parent-child attitude similarity across the life course. *J. Marriage Fam.* 991–997 (1989).

8. Ho, T. C., Sanders, S. J., Gotlib, I. H. & Hoeft, F. Intergenerational Neuroimaging of Human Brain Circuitry. *Trends Neurosci.* **39**, 644–648 (2016).

9. Flint, J., Timpson, N. & Munafò, M. Assessing the utility of intermediate phenotypes for genetic mapping of psychiatric disease. *Trends Neurosci.* **37**, 733–741 (2014).

10. Dubois, J. & Adolphs, R. Building a Science of Individual Differences from fMRI. *Trends Cogn. Sci.* **20**, 1–19 (2016).

11. Biswal, B. B. *et al.* Toward discovery science of human brain function. *Proc. Natl. Acad. Sci. U. S. A.* **107**, 4734–4739 (2010).

12. Finn, E. S. *et al.* Functional connectome fingerprinting: identifying individuals using patterns of brain connectivity. *Nat. Neurosci.* **18**, 1–11 (2015).

13. Rosenberg, M. D. *et al.* A neuromarker of sustained attention from whole-brain functional connectivity. *Nat. Neurosci.* **19**, 165–71 (2016).

14. Takagi, Y., Hirayama, J. ichiro & Tanaka, S. C. State-unspecific patterns of whole-brain functional connectivity from resting and multiple task states predict stable individual traits. *Neuroimage* **201**, 116036 (2019).

15. van den Heuvel, M. P., Stam, C. J., Kahn, R. S. & Hulshoff Pol, H. E. Efficiency of functional brain networks and intellectual performance. *J. Neurosci.* **29**, 7619–24

698         (2009).

699    16.   Fox, M. D. & Greicius, M. Clinical applications of resting state functional connectivity.
700         *Front. Syst. Neurosci.* **4**, 19 (2010).

701    17.   Takagi, Y. *et al.* A neural marker of obsessive-compulsive disorder from whole-brain
702         functional connectivity. *Sci. Rep.* **7**, 7538 (2017).

703    18.   Takagi, Y. *et al.* A common brain network among state, trait, and pathological anxiety
704         from whole-brain functional connectivity. *Neuroimage* **172**, 506–516 (2018).

705    19.   Yahata, N. *et al.* A small number of abnormal brain connections predicts adult autism
706         spectrum disorder. *Nat. Commun.* **7**, (2016).

707    20.   Kanai, R. & Rees, G. The structural basis of inter-individual differences in human
708         behaviour and cognition. *Nat. Rev. Neurosci.* **12**, 231–242 (2011).

709    21.   Busch, V., Schuierer, G., Bogdahn, U. & May, A. Changes in grey matter induced by
710         training Newly honed juggling skills show up as a transient feature on a brain-imaging
711         scan . *Nature* **427**, 311–312 (2004).

712    22.   Duncan, J. *et al.* A neural basis for general intelligence. *Science (80-. ).* **289**, 457–460
713         (2000).

714    23.   Okada, N. *et al.* Smaller anterior subgenual cingulate volume mediates the effect of
715         girls' early sexual maturation on negative psychobehavioral outcome. *Neuroimage*
716         **209**, 116478 (2020).

717    24.   Kasai, K. *et al.* Progressive decrease of left superior temporal gyrus gray matter
718         volume in patients with first-episode schizophrenia. *Am. J. Psychiatry* **160**, 156–164
719         (2003).

720    25.   Elliott, L. T. *et al.* Genome-wide association studies of brain imaging phenotypes in UK
721         Biobank. *Nature* **562**, 210–216 (2018).

722    26.   Feng, J. *et al.* Partitioning heritability analyses unveil the genetic architecture of
723         human brain multidimensional functional connectivity patterns. *Hum. Brain Mapp.*
724         (2020).

725    27.   Ge, T., Holmes, A. J., Buckner, R. L., Smoller, J. W. & Sabuncu, M. R. Heritability
726         analysis with repeat measurements and its application to resting-state functional
727         connectivity. *Proc. Natl. Acad. Sci.* **114**, 5521–5526 (2017).

728    28.   Moodie, C. A., Wisner, K. M. & MacDonald III, A. W. Characteristics of canonical
729         intrinsic connectivity networks across tasks and monozygotic twin pairs. *Hum. Brain*
730         *Mapp.* **35**, 5532–5549 (2014).

731    29.   Yang, Z. *et al.* Genetic and environmental contributions to functional connectivity
732         architecture of the human brain. *Cereb. cortex* **26**, 2341–2352 (2016).

733  30.  Sinclair, B. *et al.* Heritability of the network architecture of intrinsic brain functional
734       connectivity. *Neuroimage* **121**, 243–252 (2015).

735  31.  Xu, J. *et al.* Heritability of the effective connectivity in the resting-state default mode
736       network. *Cereb. cortex* **27**, 5626–5634 (2017).

737  32.  Fu, Y. *et al.* Genetic influences on resting-state functional networks: A twin study.
738       *Hum. Brain Mapp.* **36**, 3959–3972 (2015).

739  33.  van den Heuvel, M. P. *et al.* Genetic control of functional brain network efficiency in
740       children. *Eur. Neuropsychopharmacol.* **23**, 19–23 (2013).

741  34.  Achterberg, M. *et al.* Distinctive heritability patterns of subcortical-prefrontal cortex
742       resting state connectivity in childhood: A twin study. *Neuroimage* **175**, 138–149
743       (2018).

744  35.  Gao, W. *et al.* Intersubject variability of and genetic effects on the brain's functional
745       connectivity during infancy. *J. Neurosci.* **34**, 11288–11296 (2014).

746  36.  Teeuw, J. *et al.* Genetic and environmental influences on functional connectivity
747       within and between canonical cortical resting-state networks throughout adolescent
748       development in boys and girls. *Neuroimage* **202**, 116073 (2019).

749  37.  Glahn, D. C. *et al.* Genetic control over the resting brain. *Proc. Natl. Acad. Sci.* **107**,
750       1223–1228 (2010).

751  38.  Sudre, G. *et al.* Estimating the heritability of structural and functional brain
752       connectivity in families affected by attention-deficit/hyperactivity disorder. *JAMA*
753       *psychiatry* **74**, 76–84 (2017).

754  39.  Korgaonkar, M. S., Ram, K., Williams, L. M., Gatt, J. M. & Grieve, S. M. Establishing the
755       resting state default mode network derived from functional magnetic resonance
756       imaging tasks as an endophenotype: A twins study. *Hum. Brain Mapp.* **35**, 3893–3902
757       (2014).

758  40.  Fornito, A. *et al.* Genetic influences on cost-efficient organization of human cortical
759       functional networks. *J. Neurosci.* **31**, 3261–3270 (2011).

760  41.  Meda, S. a *et al.* Multivariate analysis reveals genetic associations of the resting
761       default mode network in psychotic bipolar disorder and schizophrenia. *Proc. Natl.*
762       *Acad. Sci. U. S. A.* **111**, E2066-75 (2014).

763  42.  Adhikari, B. M. *et al.* Comparison of heritability estimates on resting state fMRI
764       connectivity phenotypes using the ENIGMA analysis pipeline. *Hum. Brain Mapp.* **39**,
765       4893–4902 (2018).

766  43.  Colclough, G. L. *et al.* The heritability of multi-modal connectivity in human brain
767       activity. *Elife* **6**, 1–19 (2017).

768    44.    Bis, J. C., DeCarli, C., Smith, A. V & others. Common variants at 12q14 and 12q24 are
769          associated with hippocampal volume. *Nat Genet* **44**, 545–551 (2012).

770    45.    den Braber, A. *et al.* Heritability of subcortical brain measures: a perspective for
771          future genome-wide association studies. *Neuroimage* **83**, 98–102 (2013).

772    46.    Eyler, L. T. *et al.* Conceptual and data-based investigation of genetic influences and
773          brain asymmetry: a twin study of multiple structural phenotypes. *J. Cogn. Neurosci.*
774          **26**, 1100–1117 (2014).

775    47.    Blokland, G. A. M., de Zubicaray, G. I., McMahon, K. L. & Wright, M. J. Genetic and
776          environmental influences on neuroimaging phenotypes: a meta-analytical
777          perspective on twin imaging studies. *Twin Res. Hum. Genet.* **15**, 351–371 (2012).

778    48.    Kremen, W. S. *et al.* Genetic and environmental influences on the size of specific
779          brain regions in midlife: the VETSA MRI study. *Neuroimage* **49**, 1213–1223 (2010).

780    49.    Jansen, A. G., Mous, S. E., White, T., Posthuma, D. & Polderman, T. J. C. What twin
781          studies tell us about the heritability of brain development, morphology, and function:
782          a review. *Neuropsychol. Rev.* **25**, 27–46 (2015).

783    50.    Zhao, B. *et al.* Genome-wide association analysis of 19,629 individuals identifies
784          variants influencing regional brain volumes and refines their genetic co-architecture
785          with cognitive and mental health traits. *Nat. Genet.* **51**, 1637–1644 (2019).

786    51.    Ikram, M. A. *et al.* Common variants at 6q22 and 17q21 are associated with
787          intracranial volume. *Nat. Genet.* **44**, 539 (2012).

788    52.    Guadalupe, T. *et al.* Human subcortical brain asymmetries in 15,847 people
789          worldwide reveal effects of age and sex. *Brain Imaging Behav.* **11**, 1497–1514 (2017).

790    53.    Franke, B. *et al.* Genetic influences on schizophrenia and subcortical brain volumes:
791          large-scale proof of concept. *Nat. Neurosci.* **19**, 420–431 (2016).

792    54.    Hibar, D. P. *et al.* Novel genetic loci associated with hippocampal volume. *Nat.*
793          *Commun.* **8**, 1–12 (2017).

794    55.    Hibar, D. P. *et al.* Common genetic variants influence human subcortical brain
795          structures. *Nature* **520**, 224–229 (2015).

796    56.    der Meer, D. *et al.* Brain scans from 21,297 individuals reveal the genetic architecture
797          of hippocampal subfield volumes. *Mol. Psychiatry* 1–13 (2018).

798    57.    Wen, W. *et al.* Distinct genetic influences on cortical and subcortical brain structures.
799          *Sci. Rep.* **6**, 32760 (2016).

800    58.    Ge, T. *et al.* Multidimensional heritability analysis of neuroanatomical shape. *Nat.*
801          *Commun.* **7**, 1–10 (2016).

802    59.    Lee, T. H., Miernicki, M. E. & Telzer, E. H. Families that fire together smile together:

32

Resting state connectome similarity and daily emotional synchrony in parent-child dyads. *Neuroimage* **152**, 31–37 (2017).

60. Quiñones-Camacho, L. E. *et al.* Parent–child neural synchrony: a novel approach to elucidating dyadic correlates of preschool irritability. *J. Child Psychol. Psychiatry Allied Discip.* (2019). doi:10.1111/jcpp.13165

61. Reindl, V., Gerloff, C., Scharke, W. & Konrad, K. Brain-to-brain synchrony in parent-child dyads and the relationship with emotion regulation revealed by fNIRS-based hyperscanning. *Neuroimage* **178**, 493–502 (2018).

62. Yamagata, B. *et al.* Female-specific intergenerational transmission patterns of the human corticolimbic circuitry. *J. Neurosci.* **36**, 1254–1260 (2016).

63. Ando, S. *et al.* Cohort Profile: The Tokyo Teen Cohort study (TTC). *Int. J. Epidemiol.* **48**, (2019).

64. Okada, N. *et al.* Population-neuroscience study of the Tokyo TEEN Cohort (pn-TTC): Cohort longitudinal study to explore the neurobiological substrates of adolescent psychological and behavioral development. *Psychiatry Clin. Neurosci.* **73**, 231–242 (2019).

65. Shen, X., Tokoglu, F., Papademetris, X. & Constable, R. T. Groupwise whole-brain parcellation from resting-state fMRI data for network node identification. *Neuroimage* **82**, 403–415 (2013).

66. Power, J. D., Barnes, K. A., Snyder, A. Z., Schlaggar, B. L. & Petersen, S. E. Spurious but systematic correlations in functional connectivity MRI networks arise from subject motion. *Neuroimage* **59**, 2142–2154 (2012).

67. Horien, C., Shen, X., Scheinost, D. & Constable, R. T. The individual functional connectome is unique and stable over months to years. *Neuroimage* **189**, 676–687 (2019).

68. Alexander-Bloch, A., Raznahan, A., Bullmore, E. & Giedd, J. The convergence of maturational change and structural covariance in human cortical networks. *J. Neurosci.* **33**, 2889–2899 (2013).

69. Sisk, C. L. & Zehr, J. L. Pubertal hormones organize the adolescent brain and behavior. *Front. Neuroendocrinol.* **26**, 163–174 (2005).

70. Achenbach, T. M. *Child behavior checklist/4-18.* (VT: University of Vermont, 1991).

71. Petty, C. R. *et al.* The child behavior checklist broad-band scales predict subsequent psychopathology: A 5-year follow-up. *J. Anxiety Disord.* **22**, 532–539 (2008).

72. Arain, M. *et al.* Maturation of the adolescent brain. *Neuropsychiatr. Dis. Treat.* **9**, 449–461 (2013).

73.  Valizadeh, S. A., Liem, F., Mérillat, S., Hänggi, J. & Jäncke, L. Identification of individual subjects on the basis of their brain anatomical features. *Sci. Rep.* **8**, 1–9 (2018).

74.  Wachinger, C., Golland, P., Kremen, W., Fischl, B. & Reuter, M. BrainPrint: A discriminative characterization of brain morphology. *Neuroimage* **109**, 232–248 (2015).

75.  Kumar, K., Toews, M., Chauvin, L., Colliot, O. & Desrosiers, C. Multi-modal brain fingerprinting: A manifold approximation based framework. *Neuroimage* **183**, 212–226 (2018).

76.  Gennatas, E. D. *et al.* Age-related effects and sex differences in gray matter density, volume, mass, and cortical thickness from childhood to young adulthood. *J. Neurosci.* **37**, 5065–5073 (2017).

77.  Váša, F. *et al.* Conservative and disruptive modes of adolescent change in human brain functional connectivity. *Proc. Natl. Acad. Sci. U. S. A.* **117**, 3248–3253 (2020).

78.  Whitley, E., Gale, C. R., Deary, I. J., Kivimaki, M. & Batty, G. D. Association of maternal and paternal IQ with offspring conduct, emotional, and attention problem scores: Transgenerational evidence from the 1958 British birth cohort study. *Arch. Gen. Psychiatry* **68**, 1032–1038 (2011).

79.  Harden, K. P., Kretsch, N., Tackett, J. L. & Tucker-Drob, E. M. Genetic and environmental influences on testosterone in adolescents: Evidence for sex differences. *Dev. Psychobiol.* **56**, 1278–1289 (2014).

80.  Grotevant, H. D. & Cooper, C. R. Individuation in family relationships. *Hum. Dev.* **29**, 82–100 (1986).

81.  Zuo, X. N. *et al.* Human Connectomics across the Life Span. *Trends Cogn. Sci.* **21**, 32–45 (2017).

82.  Rosenberg, M. D., Casey, B. J. & Holmes, A. J. Prediction complements explanation in understanding the developing brain. *Nat. Commun.* 1–13 (2018). doi:10.1038/s41467-018-02887-9

83.  Honey, C. J. *et al.* Predicting human resting-state functional connectivity from structural connectivity. *Proc. Natl. Acad. Sci. U. S. A.* **106**, 2035–2040 (2009).

84.  Gong, G., He, Y., Chen, Z. J. & Evans, A. C. Convergence and divergence of thickness correlations with diffusion connections across the human cerebral cortex. *Neuroimage* **59**, 1239–1248 (2012).

85.  Granger, D. A., Shirtcliff, E. A., Booth, A., Kivlighan, K. T. & Schwartz, E. B. The 'trouble' with salivary testosterone. *Psychoneuroendocrinology* **29**, 1229–1240 (2004).

873  86.  Ketha, H., Kaur, S., Grebe, S. K. & Singh, R. J. Clinical applications of LC-MS sex steroid

874       assays: Evolution of methodologies in the 21st century. *Curr. Opin. Endocrinol.*

875       *Diabetes Obes.* **21**, 217–226 (2014).

876

877
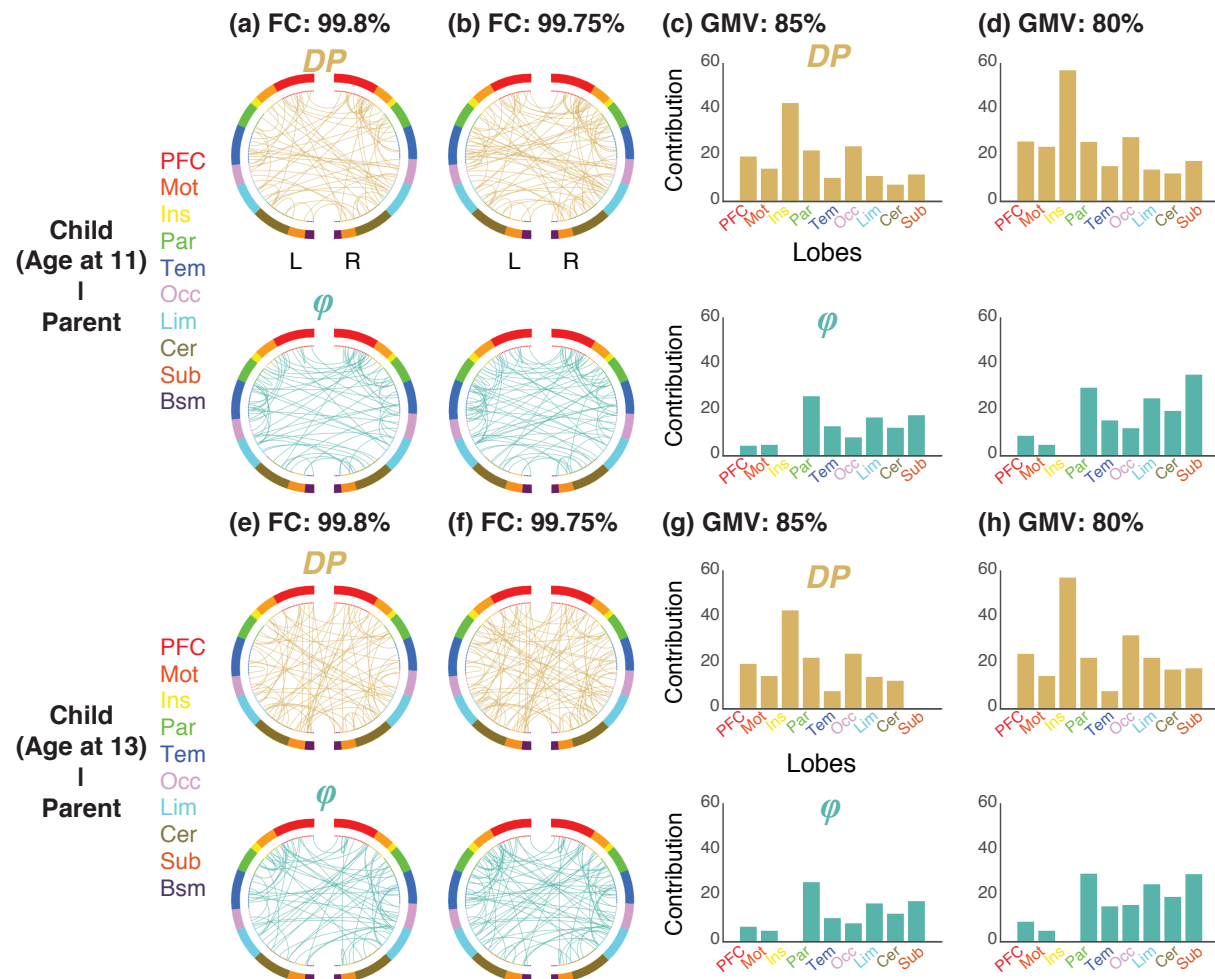
**Supplementary Figure 1**: Overall patterns of edges/regions with high differential power (highly discriminative among subjects) and group consistency (highly similar among subjects) tended to be similar across different thresholds and across development (**(a)–(d)** child at age 11); **(e)–(h)** child at age 13). The figures show the results when the edges were thresholded at the 99.8th and 99.75th percentiles for FC, and regions were thresholded at the 85th, 80th percentiles for GMV. For each threshold, a circle plot (FC) and a bar graph (GMV) are shown, in which nodes are grouped according to anatomical location.

**(a) Child (age at 11)** **(b) Child (age at 13)** **(c) Parent**
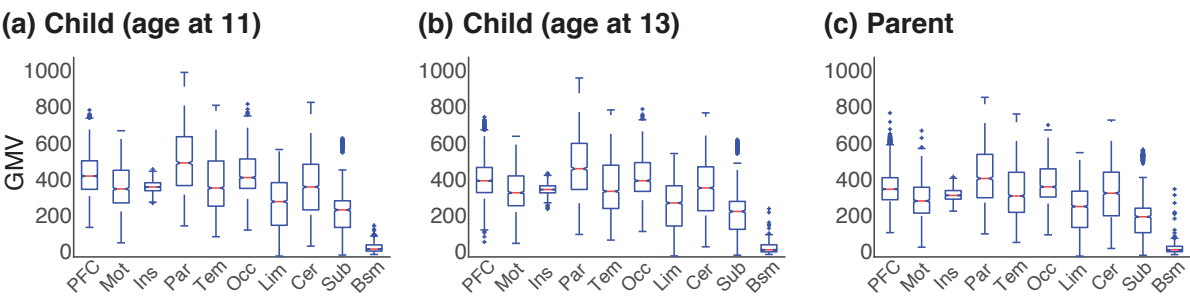


**Supplementary Figure 2**: Box plots of signal strength of each lobule for GMV. The red line indicates the median. The bottom and top edges of the box indicate the 25th and 75th percentiles, respectively. The crosses denote outliers, and the whiskers extend to the most extreme data points not considered outliers. The brainstem (the right-most boxes in each figure) exhibited much lower signal strength compared with the other lobules. Means ± s.e.m are shown.

**(a) Child (age at 11) - Parent**
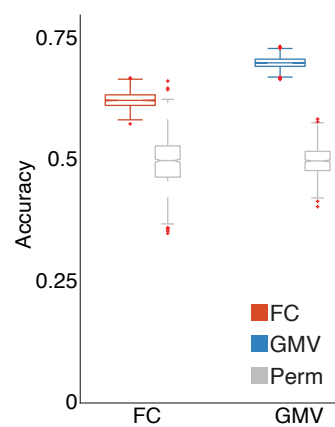


**(b) Child (age at 13) - Parent**



891
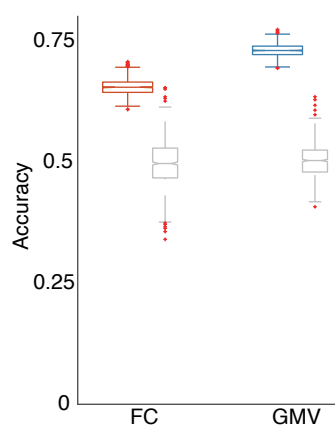
892  **Supplementary Figure 3**: Accuracies using only low-movement subjects. We confirmed that qualitatively

893  similar results were obtained when we excluded children whose head movements were in the top 25%, at

894  both age 11 and age 13, resulting in the inclusion of 41.25% of the total sample.

895
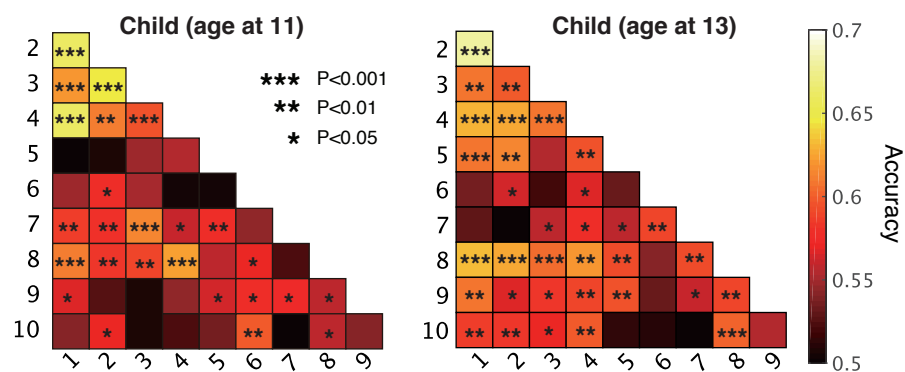
**Supplementary Figure 4**: Between-network analyses using only the between-network edges. Statistical significance was assessed by comparing the distributions for each network obtained through bootstrapping, uncorrected.
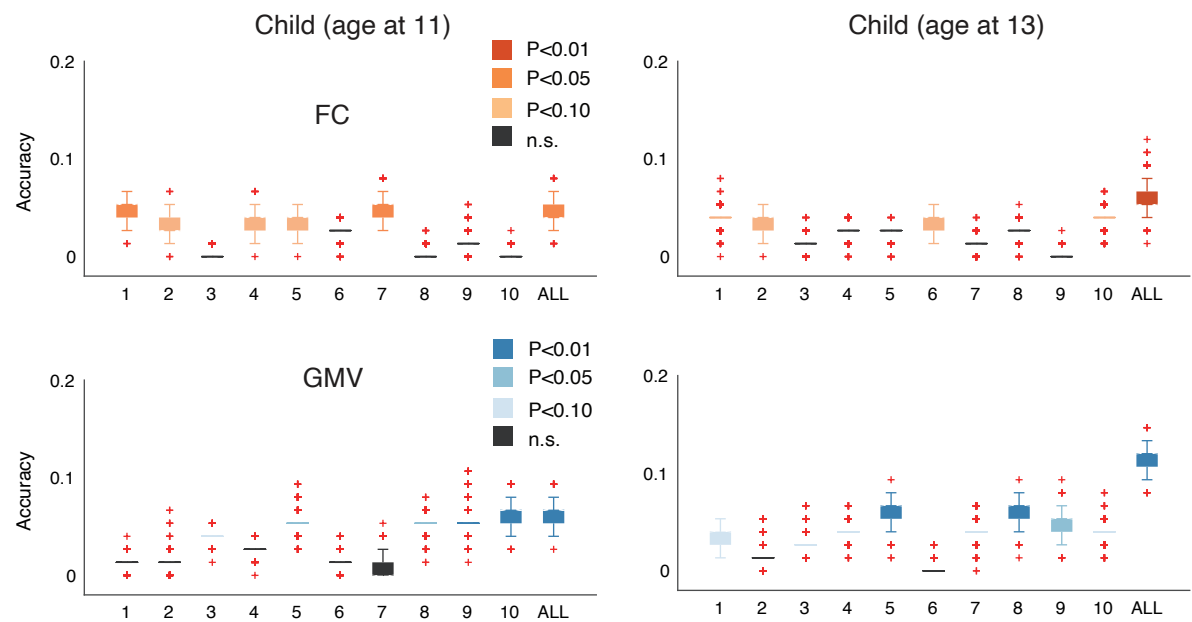
**Supplementary Figure 5:** Accuracies obtained using conventional identification methods. Box plots of accuracies using FC (top row) and GMV (bottom row) for children at age 11 (left column) and 13 (right column) are shown. The bottom and top edges of the box indicate the 25th and 75th percentiles, respectively. The crosses denote outliers, and the whiskers extend to the most extreme data points not considered outliers. n.s. non-significant.
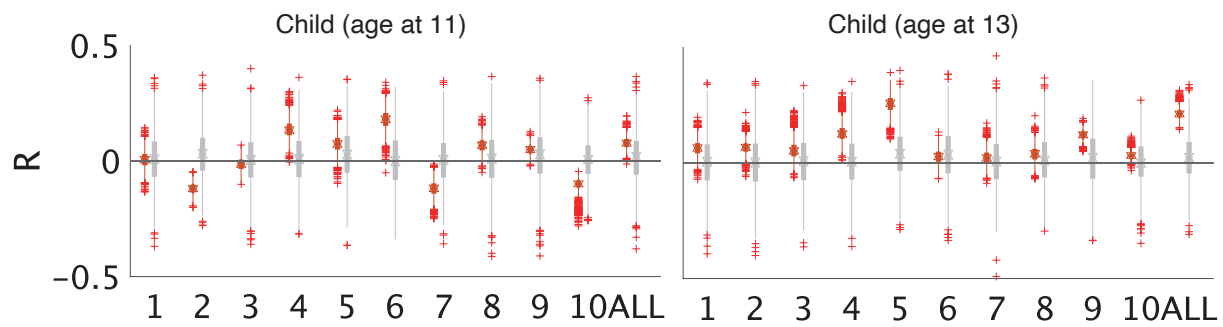
**Supplementary Figure 6** For each sub-network (1–10: sub-networks shown in Figure 3a) and whole-brain (ALL), we calculated Pearson's correlation coefficients between parent-child brain similarities defined by FC and those defined by GMV across all parent-child dyads (red box). We found that they exhibited relatively low correlations in general, suggesting that they contained independent information. Directly to the right of these red boxes (grey box) are the results of the 1,000-times permutation testing.

914
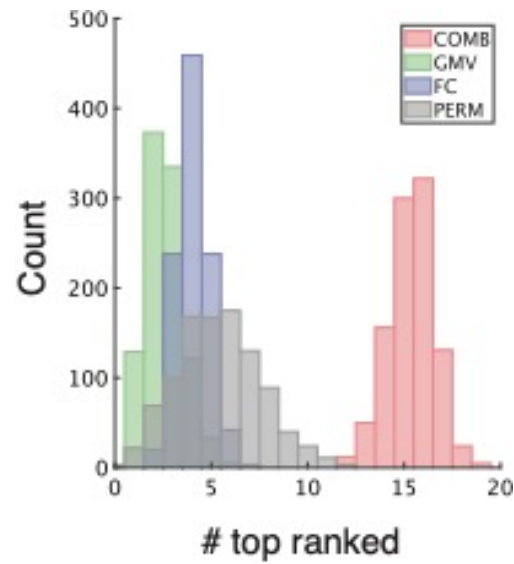
**Supplementary Figure 7:** The number of top ranked networks for COMB (red bar), GMV (green bar), and FC (blue bar) estimated via bootstrapping and null distribution (grey bar) estimated via permutation are shown.